TASK Quarterly 27 (3) 2023

Real time quantum tunneling through a double square barrier

George J. Papadopoulos[1]
Department of Physics
Solid State Physics Section
National and Kapodistrian University of Athens
Panepistimiopolis, Athens 157 84 Zografos, Athens, Greece

https://doi.org/10.34808/19qb-zg64

Abstract

The propagator of a one-dimensional double square barrier is obtained analytically in terms of the relevant eigenfunctions. With the aid of the propagator the wavefunction evolution for a particle, initially in a state of wave packet, located on the left-hand side of the barrier, with ignorable overlap with the barrier, is obtained. There follows study of the probability and current densities stemming from the particle initial state. In particular, the space distributions at given times of the above densities are given. Furthermore, their evolution in time at the entrance and exit of the barrier is obtained. The numerical results show repeated reversal in the current density at the barrier entrance, while being unidirectional at the exit. However, the probability of entering the barrier over an extremely long time tends to equal the corresponding probability of exiting the barrier. Owing to the fact that the wave packet expands on both of its sides, as time goes by, it is possible to have transmission even if the particle's initial momentum points away from the barrier. The effect, in question, becomes evident in diagrams for the transmitted probability beyond the barrier exit in terms of the particle initial momentum, over a region.

Keywords:

double square barrier propagator, probability density, current density, wave packet, transmitted probability

[1]Corresponding author. E-mail: gpapado@phys.uoa.gr

1. Introduction

In this work, we consider a set up involving a one-dimensional (1D) double square barrier together with a particle on the left approaching, or moving away, initially in a state of a Gaussian wave packet. The wave packet's location and width are such that its overlap with the barrier region is extremely negligible. There follows obtaining the evolving wave function employing the relevant propagator. From the wave function, in question, we proceed obtaining probability and current densities space - and time-wise. Actually, the present work constitutes an extension of recent work, which involves a single square barrier [1].

Treatment of time dependent scattering of Gaussian wave packets appears in the literature via numerical approach [2], also decay of wave function initially located in the well between the barriers of a double barrier is also treated numerically [3], and, also, analytically [4]. However, with employment of propagators one can handle more general cases of tunneling problems with regard to temporal as well as spatial development. Furthermore, the procedure. followed, enables estimating the time taken by a portion of the evolving wave function for complete evacuation of the barrier region to be extremely long.

In section 2 we deal with expression for the transmitted probability beyond the barrier exit making use of the time evolution of current densities at the barrier entrance or exit over extremely long times, more accurately tending to infinity. Furthermore, the spatial distribution at such long times can be employed for obtaining the transmitted probability. Section 3 deals with obtaining the required propagator, utilizing a complete set of real eigenfunctions. Section 4 provides numerical results relating to spatial distributions of probability and current densities at given times, as well as their time evolution at the barrier entrance and exit. Also, graphs for the transmitted probability in terms of the impinging particle mean initial momentum is provided for given widths of the wave packet and potential barrier parameters. Section 5 deals with conclusions.

2. Probability and current densities

In this section, we consider a one-dimensional double square barrier with potential energy

$$\begin{aligned} U(x) &= u_0[\theta(x+a+b)-\theta(x+a) \\ &\quad +\theta(x-a)-\theta(x-a-b)] \end{aligned} \tag{1}$$

where θ stands for the step function and u_0 for the barrier height, a and b are >0 and $a+b$ indicates the barrier exit, while the barrier entrance is located at $-(a+b)$ and, furthermore, $-a, a$ determine correspondingly the boundaries of the region within the left hand and right hand side barriers.

Our study involves a particle approaching the double square barrier from some distance, with ignorable overlap, initially in a wave packet state

$$\Phi(x) = \frac{1}{(2\pi s^2)^{1/4}} \exp[-\frac{1}{4s^2}(x-x_0)^2 + \frac{i}{\hbar}p_0(x-x_0)] \tag{2}$$

where x_0, p_0, and s are the wave packet center, mean momentum and mean spread.

Under the circumstances, in the course of time the wave function, stemming from the wave packet, above, initially expands on either side, but faster in the direction of the mean momentum, p_0. At some later time, the right-hand side edge of the evolving wave function reaches the barrier at the barrier entrance, $-(a+b)$, and proceeds crossing the barrier.

For obtaining the wave function, $\Psi(x,t)$, stemming from the initial wave packet, $\Phi(x)$, we have to solve the Schrödinger equation, relating to the potential energy given in Equation 1

$$\imath\hbar\frac{\partial}{\partial t}\Psi(x,t) = \left[-\frac{\hbar^2}{2m}\frac{\partial^2}{\partial x^2} + U(x)\right]\Psi(x,t) \tag{3}$$

under the condition

$$\Psi(x,0) = \Phi(x) \tag{4}$$

Details for the procedure followed for obtaining the required $\Psi(x,t)$ are provided in Section 3, based on the propagator, $K(xt|x'0)$, of the Schrödinger Equation 3.

Having at hand the wave function $\Psi(x,t)$ the probability and current densities ρ, and J, are obtained, both time– and space–wise, through the expressions:

$$\rho(x,t) = |\Psi(x,t)|^2, \quad J(x,t) = \frac{\hbar}{m}\mathrm{Im}\left[\Psi(x,t)^*\frac{\partial}{\partial x}\Psi(x,t)\right] \tag{5}$$

The time taken for the evolving wave function, $\Psi(x,t)$, to stabilize completely is essentially infinite. However, after an extremely long time the wave function changes insignificantly. On account of the wave function evolution the probability and current densities vary after extremely long time also insignificantly. The picture one gets for the current density time evolution at the barrier

entrance, $J(-a-b,t)$, is that it starts flowing into and out of the barrier repeatedly with decreasing amplitude as time goes by. On the other hand at the exit the current density, $J(a+b,t)$, gets out continuously and tends to zero after quite a long time.

In the case of time-dependent tunneling the transmitted probability, T_p, is provided by the fraction of the probability of finding the particle beyond the barrier exit after an extremely long time, essentially infinite, when the wave function gets stabilized. After such a long time the barrier region gets empty of probability. Thus, the transmitted probability can be expressed through the time evolution of the current density either at the barrier entrance or exit as

$$T_p = \int_0^\infty J(a+b,\tau)\, d\tau = \int_0^\infty J(-a-b,\tau)\, d\tau \tag{6}$$

For examples after a long time see section 4. Another way for obtaining the transmitted probability is based on the probability density established in the region beyond the barrier exit after essentially infinite time. Thus, we have:

$$T_p = \int_{a+b}^\infty \rho(x,t)\, dx \tag{7}$$

as $t \to \infty$.
It is evident, that

$$\int_{-\infty}^{-a-b} \rho(x,t)\, dx = 1 - T_p \tag{8}$$

as $t \to \infty$.
In practice one can obtain essentially accurate results for the Equations 6, 7 and 8 for extremely long times replacing the infinite limits by extremely large ones.

We close the present section with remarks concerning the plane wave structure of the initial wave packet state, which takes the form

$$\Phi(x) = \int_0^\infty G(k)\left[f(k,x) + f(-k,x)\right] dk \tag{9}$$

where $f(k,x)$ and $G(k)$ stand correspondingly for plane wave and associated amplitude, given by

$$f(k,x) = \exp\left[i\left(k + \frac{1}{\hbar}p_o\right)(x - x_o)\right] \tag{10}$$

$$G(k) = \left(\frac{s}{\pi}\right)^{1/4} \frac{1}{(2\pi)^{1/4}} \exp\left(-s^2k^2\right) \tag{11}$$

The above structure enables one to conclude the possibility of having transmission even in case whereby the wave packet's mean momentum points away from the barrier ($p_0 < 0$). Details for such an effect appear in Figures 5a and 5b. Furthermore, one can through (Equations 10 and 11) conclude an increase in transmission with a smaller wave packet width.

3. Double barrier propagator

In order to proceed for obtaining the propagator, in question, we shall presently make use of a particular complete set of eigenfunctions, namely, symmetric and antisymmetric. As we shall see, later on, these eigenfunctions are real, a fact that facilitates our evaluations. We begin with a set of non-normalized eigenfunctions described in the regions $x \le -(a+b)$, $-(a+b) \le x \le -a$, $-a \le x \le a$, and denoted, correspondingly by l_2, l_1, o, r_1, r_2.

The symmetric ones associated with the above regions take the form

$$\begin{aligned}
Y_{sl_2} &= \left[\cos(ka)\cosh(Kb) - \frac{k}{K}\sin(ka)\sinh(Kb)\right] \\
&\quad \cos[k(x+a+b)] + \\
&\quad \left[\sin(ka)\cosh(Kb) - \frac{K}{k}\cos(ka)\sinh(Kb)\right] \\
&\quad \sin[k(x+a+b)] \\
Y_{sl_1} &= \cos(ka)\cosh[K(x+a)] + \\
&\quad \frac{k}{K}\sin(ka)\sinh[K(x+a)] \\
Y_{so} &= \cos kx \\
Y_{sr_1} &= \cos(ka)\cosh[K(x-a)] - \\
&\quad \frac{k}{K}\sin(ka)\sinh[K(x-a)] \\
Y_{sr_2} &= \left[\cos(ka)\cosh(Kb) - \frac{k}{K}\sin(ka)\sinh(Kb)\right] \\
&\quad \cos[k(x-a-b)] + \\
&\quad \left[-\sin(ka)\cosh(Kb) + \frac{k}{K}\cos(ka)\sinh(Kb)\right] \\
&\quad \sin[k(x-a-b)]
\end{aligned} \tag{12}$$

The above expressions constitute symmetric eigensolutions of the Schrödinger equations associated with the continuous quantum variable $k (k > 0)$ and eigenvalue $E_k = \hbar^2 k^2/2m$. For each k there corresponds to an antisymmetric eigensolution given for the above regions as follows:

$$
\begin{aligned}
Y_{al_2} &= -\left[\sin(ka)\cosh(Kb)+\frac{k}{K}\cos(ka)\sinh(Kb)\right] \\
&\quad \cos[k(x+a+b)]+ \\
&\quad \left[\cos(ka)\cosh(Kb)+\frac{K}{k}\sin(ka)\sinh(Kb)\right] \\
&\quad \sin[k(x+a+b)] \\
Y_{al_1} &= -\sin(ka)\cosh[K(x+a)]+ \\
&\quad \frac{k}{K}\cos(ka)\sinh[K(x+a)] \\
Y_{ao} &= \sin(kx) \\
Y_{ar_1} &= \sin(ka)\cosh[K(x-a)]+ \\
&\quad \frac{k}{K}\cos(ka)\sinh[K(x-a)] \\
Y_{ar_2} &= \left[\sin(ka)\cosh(Kb)+\frac{k}{K}\cos(ka)\sinh(Kb)\right] \\
&\quad \cos[k(x-a-b)]+ \\
&\quad \left[\cos(ka)\cosh(Kb)+\frac{K}{k}\sin(ka)\sinh(Kb)\right] \\
&\quad \sin[k(x-a-b)]
\end{aligned}
\tag{13}
$$

For both symmetric and antisymmetric eigensolutions K is given by

$$
K=\sqrt{\frac{2mu_o}{\hbar^2}-k^2} \tag{14}
$$

It should be noted that (Equations 13 and 14) satisfy the continuity conditions for the wave function as well as its derivative at the barrier boundaries, $-(a+b)$, $-a$, a, $(a+b)$. Furthermore, on account of the fact that the above wave functions (Equations 12 and 13) are associated with same eigenvalue, E_k, the eigenvalues are doubly degenerate.

As pointed out, earlier, the eigensolutions (Equations 12 and 13) are not normalized. In order to proceed obtaining their corresponding normalizing factors we consider, initially, a finite range, $-L \le x \le L$. We then have for the symmetric and antisymmetric case the following normalization factors

$$
\begin{aligned}
A_s &= \left(2\int_{-L}^{-(a+b)} Y_{\mathrm{sl}_2}^2\,dx+2\int_{-(a+b)}^{-a} Y_{\mathrm{sl}_1}^2\,dx\right. \\
&\quad \left.+\int_{-a}^{a} Y_{\mathrm{so}}^2\,dx\right)^{-\frac{1}{2}}
\end{aligned}
\tag{15}
$$

$$
\begin{aligned}
A_a &= \left(2\int_{-L}^{-(a+b)} Y_{\mathrm{al}_2}^2\,dx+2\int_{-(a+b)}^{-a} Y_{\mathrm{al}_1}^2\,dx\right. \\
&\quad \left.+\int_{-a}^{a} Y_{\mathrm{ao}}^2\,dx\right)^{-\frac{1}{2}}
\end{aligned}
\tag{16}
$$

The duplication of the first two integrals on the left-hand side of the barrier is based on the symmetry of the squares of the corresponding wave functions. For obtaining the required propagator L has to be extremely large, more accurately has to tend to ∞. Since the propagator $K(xt|x'0)$ takes different forms in the various regions $i = l_2,\quad l_1,\quad o,\quad r_1,\quad r_2$ for x and x', it can be expressed, when x belongs to region i and x' to region j, as

$$
\begin{aligned}
K_{ij}(x,t\mid x'0) &= \lim_{L\to\infty}\frac{L}{\pi}\int_0^{\infty}[A_s(k,L)^2 Y_{si_i}(x)Y_{sj_j}(x') \\
&\quad +A_{si}(k,L)^2 Y_{ai_i}(x)Y_{aj_j}(x')]\exp\left[-i\frac{\hbar k^2}{2m}t\right]dk
\end{aligned}
\tag{17}
$$

Let us introduce notations for the following limits

$$
\begin{aligned}
Q_s(k) &= \lim_{L\to\infty}\frac{L}{\pi}A_a(k,L)= \\
&\quad \frac{1}{\pi}\left\{\left[\sin(ka)\cosh(Kb)-\frac{K}{k}\cos(ka)\sinh(Kb)\right]^2\right. \\
&\quad \left.+\left[\cos(ka)\cosh(Kb)-\frac{k}{K}\sin(ka)\sinh(Kb)\right]^2\right\}^{-1}
\end{aligned}
\tag{18}
$$

$$
\begin{aligned}
Q_a(k) &= \lim_{L\to\infty}\frac{L}{\pi}A_a(k,L)= \\
&\quad \frac{1}{\pi}\left\{\left[\sin(ka)\sinh(Kb)+\frac{k}{K}\cos(ka)\sinh(Kb)\right]^2\right. \\
&\quad \left.+\left[\cos(ka)\cosh(Kb)+\frac{K}{k}\sin(ka)\sinh(Kb)\right]^2\right\}^{-1}
\end{aligned}
\tag{19}
$$

In view of the above, the propagator in the region $(-\infty,\infty)$ acquires the form

$$K_{ij}\left(xt \mid x'0\right) = \int_0^{\infty}\Big[Q_s(k)Y_{si}(x)Y_{sj}(x') + Q_a(k)Y_{ai}(x)Y_{aj}(x')\Big]\exp\left(-i\frac{\hbar k^2}{2m}t\right)dk \tag{20}$$

It should be noted that the various eigenfunctions in the propagator expression are real, as earlier pointed out.

Once the propagator is made available the evolution of an initial wave function becomes attainable. Presently, we are interested in obtaining the evolution of a wave packet, $\Phi(x)$, initially located on the left-hand side of the barrier at a distance so that it overlaps with the barrier insignificantly. Its value in the barrier region being essentially zero. Under the circumstances the evolving wave function in region i can be expressed as

$$\Psi_i(x,t) = \int_{-\infty}^{-(a+b)} K_{il_2}\left(xt \mid x'0\right)\Phi(x')\,dx' \tag{21}$$

Since, $\Phi(x)$ for $x > -(a+b)$ is practically zero the integral in Equation 21 can be extended in the region from $-\infty$ to ∞. Thus, denoting by Φ_{sl_2} and Φ_{al_2}

$$\Phi_{\mathrm{sl}_2}(k) = \int_{-\infty}^{\infty} Y_{\mathrm{sl}_2}(k,x')\Phi\left(x'\right)dx' \tag{22}$$

$$\Phi_{\mathrm{al}_2}(k) = \int_{-\infty}^{\infty} Y_{\mathrm{al}_2}(k,x')\Phi\left(x'\right)dx' \tag{23}$$

we can obtain the required wave function,

$$\Psi_i(x,t) = \int_0^{\infty}\Big[Q_s(k)\Phi_{\mathrm{sl}_2}(k)Y_{\mathrm{si}}(x) + Q_a(k)\Phi_{\mathrm{al}_2}(k)Y_{\mathrm{ai}}(x)\Big]\exp\left(-i\frac{\hbar k^2}{2m}t\right)dk \tag{24}$$

for the regions $(i = l_2, l_1, o, r_1, r_2)$. Explicit expressions for Φ_{sl_2} and Φ_{al_2} are given in appendix (Section 6) through Equations 26 and 27, correspondingly.

Having at hand the evolving wave function stemming from the initial wave packet we can employing (3) obtain the probability and current densities both time- and space-wise, as well as the transmitted probability. Relevant numerical results follow in Section 4.

Prior to proceeding, further, it is worth noting that the normalizing factors, Q_s and Q_a, exhibit significant narrow peaks centered at values of k, which for $k < \sqrt{2mu_o}/\hbar$, provide the usual resonances (transmission coefficient equal to unity) appearing in the case whereby tunneling is studied with incoming and outgoing plane waves. In particular, the Q_s peaks occur at values of k associated with the symmetric eigenstates resonances, while those of Q_a with the antisymmetric ones. As is well known the peaks of the normalizing tunneling curves occur at values of k corresponding to eigenfunctions concentrated essentially within the barrier region and particularly within the well. However, such resonances do not appear in the case of a wave packet, on account of the superposition of incoming and outgoing plane waves.

4. Numerical results

In this section, we present results on the basis of which one can form a picture of the spatial distribution for the probability and current densities at given times, as well as their corresponding time evolution at the barrier entrance and exit. Furthermore, we obtain the transmitted probability as a function of the mean momentum carried by the wave packet with barrier parameters (u_0, a, b), given in data in common, which follow.

In order to proceed numerically it would be helpful to introduce as unit of energy, $E_u = 0.1eV\,(= 1.601917 \times 10^{-13}$ erg). The particular choice, in question, is based on the fact that the usual height of barriers is on the order of a few $0.1eV$. On the basis of this unit together with the carrier particle mass, m, we form the units of time, length, velocity, and momentum correspondingly as:

$$T_u = \frac{\hbar}{E_u}, \quad L_u = \frac{\hbar}{\sqrt{mE_u}}, \quad V_u = \frac{L_u}{T_u}, \quad P_u = m\frac{L_u}{T_u} = \sqrt{mE_u} \tag{25}$$

Using for m the electron mass, $m = 9.109558 \times 10^{-28}g$, and $\hbar = 1.054559 \times 10^{-27}$ erg $\cdot\, s$ for Planck's constant, the units in Equations 25 take the following values: $T_u = 6.58198 \times 10^{-15}s$, $L_u = 8.72901 \times 10^{-8}$ cm, $V_u = 1.32262 \times 10^{7}$ cm/s, $P_u = 1.20811 \times 10^{-20}$ g $\cdot$ cm/s.

The above system of units enables dealing with dimensionless quantities, just by setting in Schrödinger's Equation 3 $\hbar = 1$, $m = 1$. The various dimensional results are obtained from the resulting dimensionless quantities times their associated units, given in Equations 25. Utilizing the procedure, in question, we can obtain via Equation 24 the required wave function $\Psi_i(x,t)$ from which we derive probability and current densities, ρ and J, through Equation 5, as well as transmitted probability, T_p, using either Equation 6 or Equation 7.

In the ensuing results, we make use of data in common with regard to the barrier potential being $u_0 = 5E_u$,

$a = 2L_u$, $b = 1L_u$. The parameters x_0 and p_0 and s for the wave packet can be varied and are given in the corresponding figure captions.

The figures below refer to the probability and current densities. In particular, Figure 1a depicts initial probability density space distribution (solid curve) as well as the form it takes after a short time, $1T_u$, (dashed curve). Figure 1b provides the corresponding spatial distributions of the current densities. Subsequently, Figures 2a, 2b show correspondingly probability and current densities at $t = 8T_u$.

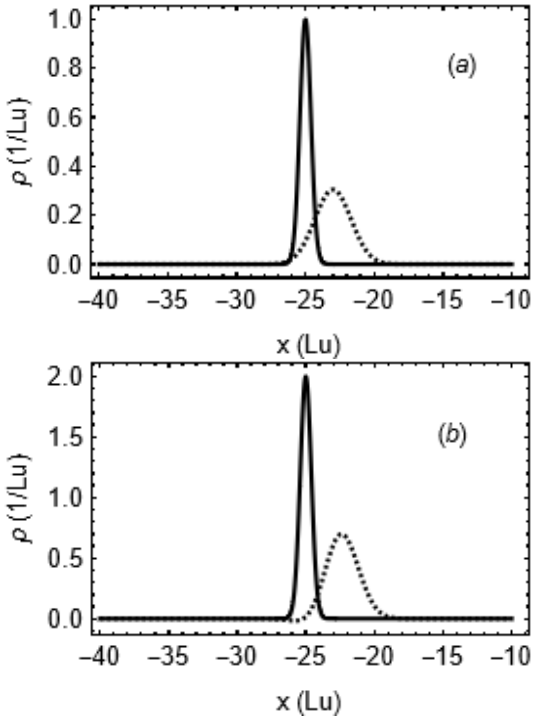

Figure 1: (a) Probability density spatial distributions emanating from an initial wave packet with width $s = 0.4L_u$. centred at $x_0 = -25L_u$ and currying mean momentum $p_0 = 2P_u$ at time $t = 0$ (solid curve) and at $t = 1T_u$ (dashed curve). The rest of the data as in common. (b) Corresponding current spatial density at time $t = 0$ (solid curve) and at $t = 1T_u$ (dashed curve).

Results concerning time evolution of probability and current densities at the barrier entrance are presented in Figures 3a, 3b, while corresponding results are shown in Figures 4a, 4b at the exit. In what concerns the current density at the entrance there appears successive change in the current direction, while at the exit current gets out continuously. Evidently, the more away from barrier the location of the initial wave packet the longer it takes for the probability and current densities to start and get established.

The figures, which follow, depict the transmitted probability as a function of the mean momentum curried by the initial wave packet. Clearly, one notices transmission in case the mean momentum points away from the barrier. It should be noted that through pertinent calculations it is verified that the transmitted probability does not depend on the initial wave packet location.

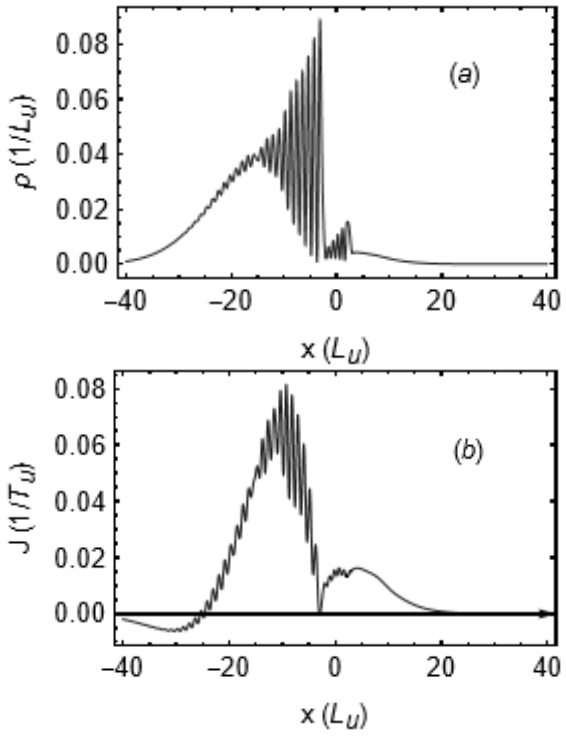

Figure 2: Probability density spatial distribution at $t = 8T_u$ emanating from an initial wave packet located at $x_0 = -25L_u$ and carrying a mean momentum $p_0 = 1.5P_u$, and width $s = 0.4L_u$. The rest of the data as per Figure 1a, (b) Corresponding current density spatial distribution

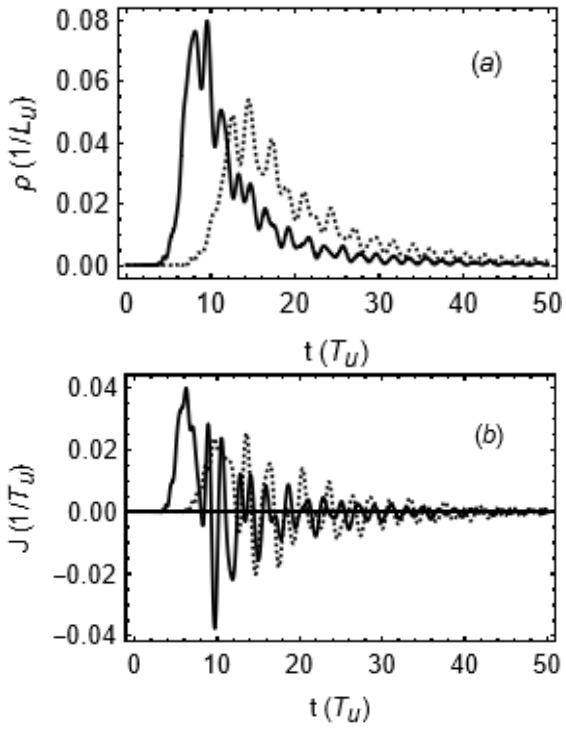

Figure 3: (a) Probability density time evolution at the barrier entrance, $x = -(a+b) = -3L_u$, resulting from initial wave packet with mean momentum $p_0 = 1.5P_u$, centred at $x_0 = -25L_u$ with width $s = 0.4L_u$(solid curve), and at $x_0 = -40L_u$ (dashed curve). The rest of the data those in common. (b) Depicts the corresponding current densities.

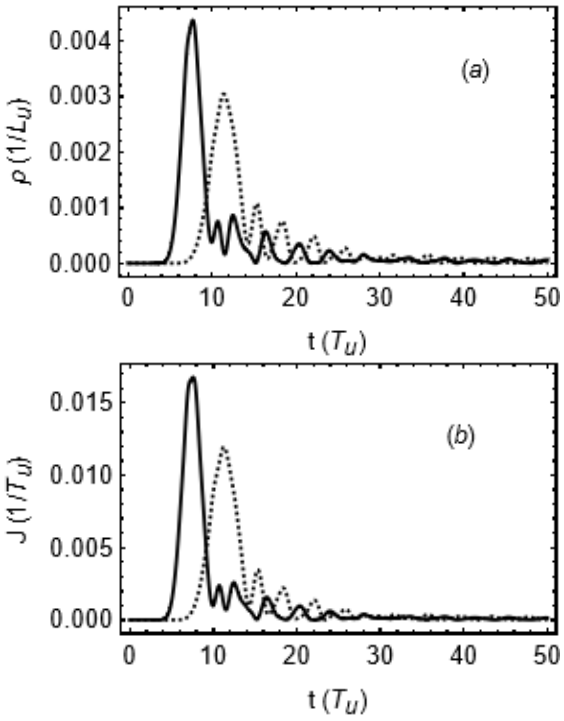

Figure 4: (a) Probability density evolutions at the barrier exit, $x+a+b=3L_u$, associated with data as per Figure 3a. (b) Corresponding current density time evolutions.

5. Conclusion

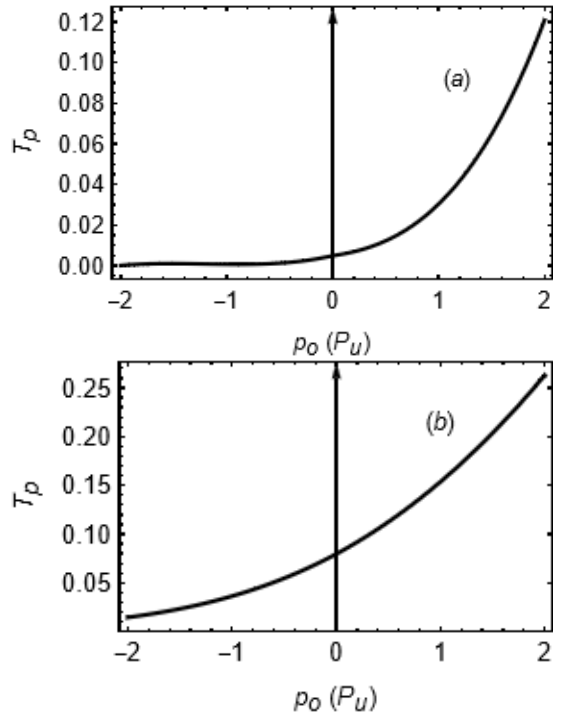

Figure 5: (a) Transmitted probability versus mean momentum carried by the initial wave packet located at $x_0=-30L_u$, $s=0.4L_u$, (b) Corresponding result associated with width $s=0.2L_u$. The rest of the data those as in common.

In conclusion we may accentuate the following remarks from the above study, particularly: i) Independence of the transmitted probability, from a given wave packet, on the initial location, provided its overlap with the barrier region is negligible. The further away the initial location from the barrier it takes longer for the transmission to get started. However, for smaller wave packet width the transmitted probability becomes larger. ii) The current density at the barrier entrance starts by getting into and out of the barrier repeatedly over a long time until it essentially nullifies, while it exits the barrier unidirectionally. Over extremely long time the probability entering the barrier, equals the one exiting the barrier. Furthermore, the transmitted probability can be obtained either from the probability entering the barrier, which tends to equal the one exiting the barrier over an extremely long time. At such a long time the transmitted probability can be, also, obtained from the transmitted spatial distribution. iii) There appears probability transmission through the barrier even if the initial wave packet mean momentum points away from the barrier.

6. Appendix

There follow corresponding analytical expressions for the integrals in Equation 22 and Equation 23

$$\begin{aligned}\Phi_{\mathrm{sl}_2}(k) \;=\; & \left(\frac{\pi}{2}\right)^{\frac{1}{4}}\sqrt{s}\\ & \left\{\left[\cosh(Kb)e^{-\imath ka}+\left(\imath\frac{K}{k}\cos(ka)-\frac{k}{K}\sin(ka)\right)\right.\right.\\ & \left.\sinh(Kb)\right]\exp\left[-s^2\left(k+\frac{p_o}{\hbar}\right)^2+ik(x_o+a+b)\right]\\ & +\left[\cosh(Kb)e^{\imath ka}-\left(\imath\frac{K}{k}\cos(ka)+\frac{k}{K}\sin(ka)\right)\right.\\ & \left.\left.\sinh(Kb)\right]\exp\left[-s^2\left(k-\frac{p_o}{\hbar}\right)^2-ik(x_o+a+b)\right]\right\}\end{aligned} \tag{26}$$

$$
\begin{aligned}
\Phi_{\mathrm{al}_2}(k) \quad = \quad & \left(\frac{\pi}{2}\right)^{\frac{1}{4}} \sqrt{s} \\
& \left\{ \left[-\imath \cosh(Kb) e^{\imath ka} - \left(\frac{k}{K} \cos(ka) + \imath \frac{K}{k} \sin(ka) \right) \right. \right. \\
& \left. \sinh(Kb) \right] \exp\left[-s^2 \left(k + \frac{p_o}{\hbar} \right)^2 + ik(x_o + a + b) \right] \\
& + \left[\imath \cosh(Kb) e^{\imath ka} - \left(\frac{k}{K} \cos(ka) - \imath \frac{K}{k} \sin(ka) \right) \right. \\
& \left. \left. \sinh(Kb) \right] \exp\left[-s^2 \left(k - \frac{p_o}{\hbar} \right)^2 - ik(x_o + a + b) \right] \right\}
\end{aligned}
\tag{27}
$$

References

[1] G. J. Papadopoulos, "Real time quantum tunneling," *TASK Quarterly. Scientific Bulletin of Academic Computer Centre in Gdansk*, vol. 19, no. 1, pp. 65–74, 2015.

[2] V. Petrillo and V. Olkhovsky, "Tunnelling time of a gaussian wave packet through two potential barriers," *Central European Journal of Physics*, vol. 3, no. 3, pp. 339–350, 2005.

[3] H. Guo, K. Diff, G. Neofotistos, and J. Gunton, "Time-dependent investigation of the resonant tunneling in a double-barrier quantum well," *Applied physics letters*, vol. 53, no. 2, pp. 131–133, 1988.

[4] S. Cordero and G. Garcia-Calderon, "Transient effects and reconstruction of the energy spectra in the time evolution of transmitted gaussian wave packets," *Journal of Physics A: Mathematical and Theoretical*, vol. 43, no. 18, p. 185301, 2010.